Applied Clay Science 182 (2019) 105294

Contents lists available at ScienceDirect

Applied Clay Science

journal homepage: www.elsevier.com/locate/clay

Research paper

Kaolin-supported ZnO nanoparticle catalysts in self-sensitized tetracycline photodegradation: Zero-point charge and pH effects

Ahed H. Zyoud[a,*], Amani Zubi[a], Samer H. Zyoud[b], Muath H. Hilal[c], Shaher Zyoud[d], Naser Qamhieh[e], AbdulRazack Hajamohideen[e], Hikmat S. Hilal[a]

[a] SSERL, Department of Chemistry, An-Najah National University, Nablus, Palestine
[b] Department of Mathematics and Basic Science, Ajman University, United Arab Emirates
[c] College of Pharmacy and Nutrition, University of Saskatchewan, 116 Thorvaldson Building, Saskatoon S7N 5C9, Canada
[d] Department of Building Engineering, Palestine Technical University (Kadoorie), Palestine.
[e] Department of Physics, United Arab Emirates University, Al-Ain, United Arab Emirates

ARTICLE INFO

Keywords:
Kaolin supported ZnO
Tetracycline
Photodegradation
Zero point charge
Sensitization

ABSTRACT

Natural waters are prone to pollution with organic contaminants, waste pharmaceuticals being an example. Pharmaceutical compounds are widely detected in different surface waters, such as lakes and rivers. Removal of such contaminants from water is therefore imperative. Different strategies are commonly followed such as adsorption, chlorination, ozonation, peroxidation and others. Each method has its shortcomings. Photodegradation of water organic contaminants by semiconductors is a safe and non-costly method. In photodegradation, the organic contaminant is completely mineralized with radiation and oxygen using stable semiconductor nanoparticles as photocatalysts. ZnO nanopowder is widely described for photodegradation processes. Due to its wide band gap (~3.2 eV) ZnO excitation is limited to UV radiation. Moreover, the nano-particle nature for the ZnO catalyst makes it difficult to recover and re-use after process completion. Supporting the ZnO nanoparticles onto stable solid material surfaces is one possible way out, and is studied here. Raw clay (kaolin) is described to support ZnO particles in photodegradation of a widely encountered pharmaceutical contaminant, tetracycline (TC). The results show the possibility of annealed ZnO/Kaolin to remove TC from water, firstly by adsorbing the contaminant then by photodegrading it into mineral species. The study shows that TC molecules pre-adsorbed onto ZnO/Kaolin were mineralized during photodegradation experiments. Complete mineralization of reacted contaminant molecules was confirmed by spectrophotometry, high performance liquid chromatography (HPLC) and total organic carbon (TOC) study. Control experiments with a cut-off filter (400 nm and shorter) confirmed the ability of the catalyst to function in the visible region, where contaminant molecules behave as sensitizers in the photodegradation process. Optimizing the efficiency of the ZnO catalyst in TC photodegradation processes by studying the effect of pH using the point of zero charge (pH_{PZC}) concepts is achieved. Collectively, the results show the possibility to prepare an efficient recoverable ZnO/Kaolin catalyst, which can be sensitized with TC molecules themselves with optimal working pH range 6–9.

1. Introduction

Solar driven photodegradation of water-organic contaminants is a potentially useful method for future water purification (Hilal et al., 2009; Ruiz-Hitzky et al., 2019; Yogendra et al., 2011; Zyoud et al., 2011; Zyoud et al., 2010). In this method, low cost safe and stable semiconducting nanoparticles are used as a catalyst. The most commonly used semiconductors for these purposes are TiO_2 and ZnO (Chantes et al., 2015; Choudhury et al., 2012; Wang et al., 2016; Zyoud et al., 2016a; Zyoud et al., 2015; Zyoud and Hilal, 2009; Zyoud et al., 2010). With a band gap ~3.2 eV, these semiconductors need the UV fraction (~6%) of incident solar radiation (Moan, 2001). Compared to TiO_2, ZnO shows higher absorptivity in that region (Sakthivel et al., 2003), with superior efficiency in photodegradation processes under sunlight (Sakthivel et al., 2003; Yogendra et al., 2011). Semiconductor nanoparticle catalyst recovery is another limitation in photodegradation processes (Santhosh et al., 2018). Solid substrates like silica (Szabó et al., 2003), glass (Umar et al., 2009) or clays (montmorillonite,

* Corresponding author.
E-mail addresses: ahedzyoud@najah.edu (A.H. Zyoud), amaniz@najah.edu (A. Zubi), s.zyoud@ajman.ac.ae (S.H. Zyoud), muath456@yahoo.com (M.H. Hilal), shaher.zyoud@ptuk.edu.ps (S. Zyoud), nqamhieh@uaeu.ac.ae (N. Qamhieh), razack003@uaeu.ac.ae (A. Hajamohideen), hshilal@najah.edu (H.S. Hilal).

https://doi.org/10.1016/j.clay.2019.105294
Received 28 July 2019; Received in revised form 3 September 2019; Accepted 4 September 2019

kaolinite, and illite) were described as supports for ZnO particles (Deepracha et al., 2019; Ju et al., 2018; Ruiz-Hitzky et al., 2019; Zyoud et al., 2017; Zyoud et al., 2019). Attaching the ZnO nanoparticles onto a solid substrate facilitates catalyst recovery. The substrate may also enhance contaminant adsorption and consequently speed up the photodegradation processes. Kaolinite support, for instance, enhanced ZnO efficiency in photodegradation of aqueous 2-chlorophenol under sunlight (Kuo and Liao, 2006; Zyoud et al., 2019) and affected stability under various conditions. Montmorillonite support enhanced ZnO nanoparticle catalytic photodegradation of aqueous tetracycline degradation (Zyoud et al., 2017).

In this study, low cost naturally abundant raw clay will be assessed as support for ZnO nanoparticles. The ZnO/Clay composite will be used as a catalyst for photodegradation of aqueous tetracycline. Catalyst composite system surface charge, which may affect the photodegradation process (Liu et al., 2017; Xiang et al., 2013) will also be given special attention. The optimal adsorption condition, where the solid surface and the contaminant molecules have opposite charges, will be described. The catalyst surface charge is affected by pH (Ashraf et al., 2018), and the point of zero charge can be determined by pH drift method (Nasiruddin Khan and Sarwar, 2007). Effect of clay support high specific surface area (Diamond and Kinter, 1956) on the photodegradation process will also be investigated, taking into consideration effect of pH on contaminant adsorption behaviours of the clay, the ZnO and the ZnO/Clay.

A pharmaceutical contaminant (Tetracycline, TC) has been chosen here as target contaminant. TC is a heavily used antibiotic (Hamilton and Rowley, 2009; Organization, 2015). The drug is partly eliminated in human and animal urines and faeces in its unchanged form (Agwuh and MacGowan, 2006), and can thus reach the environment. Contamination of soil, aquatic environment (Kümmerer, 2009), wastewater and sediments (Miao et al., 2004; Xu and Li, 2010) is documented. Therefore, complete removal of TC, as a model pharmaceutical contaminant, from drinking water is imperative. TC may exist in four different structures equilibrated with three pK_a values, depending on pH value, as shown in Scheme I. Therefore, investigating the pH and point of zero charge effects on ZnO photocatalyst efficiency is the major goal of this work. TC solutions have a yellow color, the intensity of which depends on pH. Due to their wide band gap (~3.2 eV) ZnO particles demand relatively short wavelength (~387 nm or less) photons to function as photocatalysts (Choudhury et al., 2012). Such wavelengths may not be highly abundant in reaching solar radiation, only ~6% UV radiations (Kumar and Häder, 1999; Moan, 2001). This may limit the catalytic efficiency of ZnO nanoparticles in solar driven photodegradation processes (Chantes et al., 2015). However, as TC molecules absorb in the visible light, their ability to sensitize the ZnO particles will be studied here. If visible light, a major part of solar radiation, can drive photodegradation of aqueous TC molecules, then the process would have special value in water purification (Zyoud et al., 2017).

Therefore, the goal of the present study is manifold. Studying the effect of pH on adsorption and photodegradation of TC contaminant, by raw clay supported ZnO, is a major objective. Ability of TC to sensitize ZnO particles in its own photodegradation by visible light is another objective. Effect of the clay support on ZnO photocatalytic efficiency in TC mineralization is studied. Moreover, recovery of the supported ZnO catalyst, and reuse in TC photodegradation has also been investigated. To our knowledge, similar studies have not been reported earlier.

2. Materials and methods

2.1. Materials

Common lab and starting chemicals, such as zinc acetate and NaOH were purchased from Sigma-Aldrich. Raw clay paste was collected from Jaba' region (GPS coordinate: 32°19'26"N, 35°13'20"E), in the Northern parts of Palestine. The clay predominantly involves kaolinite, as confirmed by XRD patterns below, and is thus termed kaolin throughout this work. The contaminant understudy, TC hydrochloride, TC, was kindly donated by Birzeit-Palestine Pharmaceutical Co. in a pure powder form.

2.2. Equipment

A Shimadzu UV-2101PC research spectrophotometer was used to measure electronic absorption spectra. An ICE 3000 Atomic Absorption Spectrometer (AAS) was used to determine amounts of Zn supported on clay and for raw clay elemental analysis composition. A 1525 Binary Waters HPLC system was used for TC analysis. A PANalytical X'Pert PRO X-ray diffractometer (XRD), with Cu Ka (λ = 1.5418 Å), available in the laboratories of UAEU, was used for X-ray diffraction (XRD) patterns for ZnO, kaolin, and ZnO/Kaolin. A Jeol-EO Scanning Electronic Microscope, available in the laboratories of UAEU, was used for scanning electron microscopy (SEM) measurements. A 250 W Xenon halogen lamp was used as a source of solar simulated light. A LUX-meter

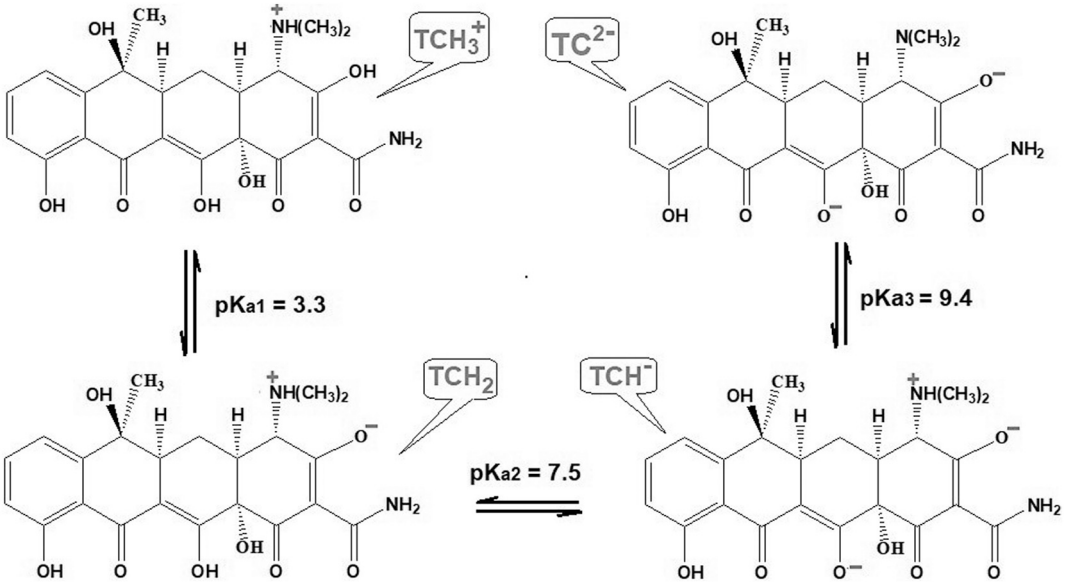

Scheme I. Effect of pH on tetracycline charge. Different equilibrium structures for tetracycline are shown with different pK_a values.

(LX-102 lightmeter) was used for measuring the light intensity that reaches the reaction surface (0.0146 W/cm^2). Thermal gravimetric analysis (TGA) was performed on a TGA-1000 Thermogravimetric analyser S. No. TGA 18001, Model BATGA by Basar Agir Makina San.

2.3. ZnO nanoparticle preparation

ZnO nanoparticles were prepared as described earlier (Zyoud et al., 2017): Aqueous NaOH solution (250.0 mL, 0.90 M) was heated to ~55 °C in a 500 mL flask. Aqueous zinc acetate solution (250.0 mL, 0.45 M) was dropwise added to the heated NaOH solution with continued magnetic stirring. The resulting ZnO white powder was decanted and washed with freshwater many times to remove any free ions. The ZnO dispersion was centrifuged at 5000 rpm for 6 min, where the white solid was dried at ~120 °C for 4 h, annealed at 450 °C under air for an hour, cooled to room temperature, crushed, sieved to size fraction < 25 μm (550 mesh) and stored under dry conditions for further use.

2.4. ZnO/Kaolin composite preparation

2.4.1. Kaolin solid preparation

A 50.0 g raw clay sample was soaked in HCl (250.0 mL, 2 M) for an hour to dissolve any undesirable soluble contents. The mixture was filtrated, and the clay sample was washed with distilled water many times until neutral. The clay was left to dry under air to get clay paste. The clay paste was dried at 120 °C for 4 h to evaporate the water content. Out of 10 g clay paste, 7.3 g resulted as dried clay. Elemental analysis and TGA analysis were performed on the dry clay sample (dried at 120 °C).

A sample of dry raw clay was annealed at 450 °C for an hour, crushed, sieved to size fraction < 25 μm (550 mesh), the produced kaolin was stored for comparison. TGA analysis was performed on the kaolin (pre-annealed at 450 °C).

2.4.2. ZnO/Kaolin preparation

The ZnO/Kaolin composite was prepared as follows. A clay paste (before drying), sample (10.0 g) was suspended in a magnetically stirred NaOH solution (250.0 mL, 0.90 M) 55 °C. After 2 h, zinc acetate solution (250.0 mL, 0.45 M) was drop-wise added to the stirred hot clay suspension. The resulting ZnO/Clay powder was decanted and washed with fresh water many times to remove any free soluble ions. The wet composite ZnO/Clay system was dried with continuous mechanical stirring in a heated mantle at 120 °C. The composite system was then annealed at 450 °C for an hour. The produced ZnO/Kaolin composite was crushed, sieved to size fraction < 25 μm (550 mesh) and stored for catalysis. To determine the ZnO percentage in the ZnO/Kaolin composite, a 0.10 g sample of the ZnO/Kaolin composite was heated in HCl (10.0 mL, 12 M). The supported ZnO was dissolved into soluble Zn^{2+} ions. The resulting solution was then diluted and analysed by AAS.

2.5. Specific surface area determination

The specific surface areas, for the pre-annealed solids ZnO, kaolin and ZnO/Kaolin, were estimated using acetic acid adsorption method, as described earlier (Adamson and Gast, 1967; Shoemaker et al., 1996).

2.6. Point of zero charge (pH_{pzc}) and surface charge determination

The pH drift method was used to determine pH_{pzc} value for the three prepared pre-annealed solids ZnO, kaolin and ZnO/Kaolin composite, as described earlier (Noh and Schwarz, 1989). A solution of 0.01 M NaCl solution was boiled to remove any dissolved CO_2 and was then kept to cool to 25 °C under nitrogen gas (99.999%) atmosphere. Three sets of six bottles were filled with 50.0 mL of the NaCl solution, each with 50.0 mL, and each adjusted to pH values (2, 4, 6, 8, 10 and 12) at 25 °C. All solutions were purged with nitrogen for 5 min, and the pH values were then measured again and assigned as initial pH values. ZnO (0.10 g) was added to each bottle of set number 1, set number 2 were charged with kaolin (0.10 g) each, while set number 3 were charged with ZnO/Kaolin. The bottles were shaken at 25 °C for 24 h. The dispersions were then left to settle and the pH was determined and assigned as final pH.

2.7. Clay elemental analysis, porosity and TGA determination

Elemental analysis was performed using AAS, for both dried clay (120 °C) and annealed (450°) kaolin samples, as described earlier (Osabor et al., 2009). A 1.00 g sample of the kaolin was digested in a clean polypropylene bottle using a mixture of concentrated HCl (~12 M) and HF (~22 M) with ratio 7:1, respectively. The mixture was heated in a thermostated water bath at ~60 °C for 2 h. The resulting milky solution was cooled in a tightly stoppered bottle under tap water, and 10.0 mL of saturated boric acid solution was then added. The mixture was covered and heated in water bath at ~70 °C until a clear solution was obtained. The clear solution was then diluted to 250.0 mL with distilled water in a plastic volumetric flask. Standard solutions and aliquots of the diluted clear digest were used for elemental analysis (Osabor et al., 2009).

The pre-annealed kaolin porosity was measured by finding the volume of absorbed water in specific volume of kaolin pieces. Details of porosity determination were described earlier (Franklin, 1979).

TGA analysis was performed for dried and pre-annealed samples. The samples were heated from room temperature to 900 °C at a ramp rate 20 °C/min under air atmosphere.

2.8. Adsorption and photocatalysis experiments

Photocatalysis experiments were always performed after adsorption equilibria were reached after 120 min. All experiments were conducted at 25 ± 1 °C.

TC adsorption capacity values for different pre-annealed solid materials ZnO, kaolin and ZnO/Kaolin at different pH values were studied. A set of TC solutions (100.0 mL, 120 ppm) were adjusted to specific pH values (3.1, 5.5, 7.2, 8.8 and 11.3). A solid material sample (0.20 g) was added to the solution with continued magnetic stirring for 120 min. Aliquots were syringed out of the reaction mixture with time and carefully double-centrifuged (5000 rpm for 3 min). The supernatants were then analysed for remaining un-adsorbed TC, and the adsorbed amounts were calculated.

Photodegradation was then started by exposing the reaction mixture from the top to solar simulated light (0.0146 W/cm^2) for additional 90 min. The mixture was kept under continued magnetic stirring during the photodegradation experiment. Aliquots were syringed out with time, doubly centrifuged and the supernatant was analysed for remaining TC using a reversed-phase HPLC method. The analyses were carried out using the mobile phase, phosphate buffer (0.01 M, pH 2.5)-acetonitrile (80:20; *v*/v), on a C18 column (250 × 4.6 mm i.d., 5 μm) at a flow rate of 1.0 mL/min, with detection at 280 nm (Hussien, 2014).

Control experiments were conducted using a cut-off filter that blocks 400 nm and shorter radiations. This was to check for possible self-sensitization of the TC for ZnO nanoparticles in photodegradation under visible irradiation. The remaining un-reacted TC was HPLC analysed.

TC desorption experiments were conducted to check for any remaining adsorbed (none-degraded) molecules on the catalyst surface after photodegradation experiments. Desorption was performed on pre-annealed solid systems ZnO, kaolin and ZnO/Kaolin. The reaction mixture was decanted, and to the solid were added dimethyl sulfoxide DMSO (20.0 mL). The mixture was then shaken for 60 min to desorb any adsorbed non-degraded TC molecules if any. The resulting liquid phase was then centrifuged and HPLC analysed for TC.

In a typical adsorption/photodegradation experiment, the TC

solution (100.0 mL, 120 ppm) was adjusted to pH ~8.8, and the catalyst ZnO/Kaolin (0.20 g) was added with stirring for 120 min in the dark to reach adsorption equilibrium. The mixture was then exposed to solar simulated light for additional 90 min. Aliquots were syringed out periodically with time during the experiments and centrifuged. The supernatants were analysed for remaining TC (or other possible organic side products) using HPLC, UV–Visible spectrophotometry and TOC analysis.

3. Results and discussion

3.1. Solid material characterization

The three pre-annealed solid systems, ZnO, kaolin and ZnO/Kaolin, were characterized using different methods. The specific surface areas for the solid systems were 14, 360 and 340 m^2/g for ZnO, kaolin and ZnO/Kaolin, respectively. The ZnO particles lowered the kaolin specific surface area by partially blocking its pores. The mass% of ZnO in the composite system was ~34%.

3.1.1. XRD patterns

The XRD patterns measured for pre-annealed solid systems ZnO, kaolin and ZnO/Kaolin are shown in Fig. 1. The Wurtzite phase is confirmed for the ZnO powder by comparison with reference card (JCPDS-79-2205) for ZnO. Based on Scherrer equation calculations using, 100, 002, and 101 reflections, the average particle size was ~30 nm. Calculations were based on shape factor value =1, because the ZnO particles assume approximately spherical shapes as observed from enlarged SEM images, vide infra.

The presence of ZnO particles, in their wurtzite phase, with an average size of 26 nm, is also confirmed in ZnO/Kaolin. The clay-supported ZnO particles were smaller than un-supported ones due to their attachment at the clay surface that prevents more particle growth. XRD patterns for ZnO/Kaolin and for kaoin also confirm the presence of kaolinite (JCPDS card No. 89-6538) as a major phase, montmorillonite (JCPDS card No. 13-135) and to a lesser extent and quartz (JSPDS card No. 89-8934), in congruence with earlier reports for raw clay (Hadjltaief et al., 2014; Morkel et al., 2006; Zyoud et al., 2016b). Therefore, the clay used in this study is considered as kaolin.

3.1.2. Solid state electronic absorption spectra

Solid state UV–visible spectra for the solids ZnO powder, kaolin, and ZnO/Kaolin were measured as aqueous dispersions (0.10 g in 50.0 mL). The spectra for all three solids are shown in Fig. 2, using aqueous background. A typical absorption maximum at ~385 nm in congruence with earlier reports (Zyoud et al., 2017) is shown in ZnO spectrum. The kaolin showed small absorption maximum at ~300 nm. The ZnO/Kaolin composite showed an absorption maximum at ~385 nm for the supported ZnO particles, with a shoulder at ~300 nm for the kaolin support. Absorption maxima of ZnO at ~380 nm proved that the ZnO particles may be excited by the UV radiations is only.

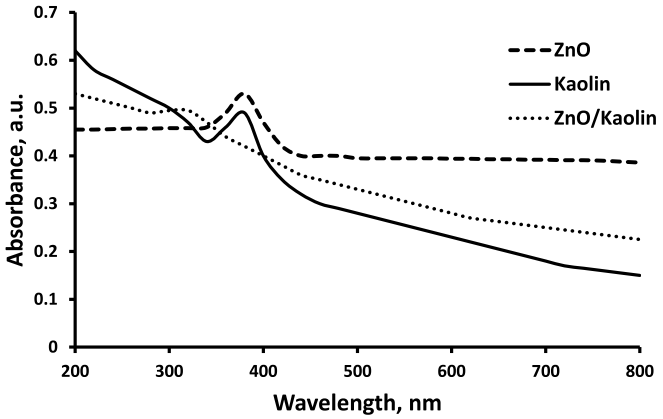

Fig. 2. Solid state electronic absorption spectra measured for pre-annealed ZnO powder, kaolin and ZnO/Kaolin. All measurements were made as aqueous dispersions of 0.1 g in 50 mL distilled water. Baseline correction was made with distilled water.

3.1.3. SEM results

SEM micrographs, measured for pre-annealed systems ZnO, kaolin and ZnO/Kaolin are shown in Fig. 3. In Fig. 3a the kaolin powder appeared as agglomerates of sheets. The agglomerate sizes are in the range 0.2–4.0 μm. Agglomerates (~200 nm) of ZnO that involve smaller nanoparticles (~30 nm calculated from XRD) are shown in Fig. 3b for the unsupported powder. Fig. 3c confirmed the presence of ZnO nanoparticles (~26 nm) attached to the clay powder surfaces in the ZnO/Kaolin. Expansion of SEM images confirms that the ZnO particles have approximately spherical shapes, as described in supplementary Fig. S1.

3.1.4. Results of pH_{pzc}

Plots of Δ(pH) vs. pH for pre-annealed solids ZnO, kaolin and ZnO/Kaolin solids were constructed and are described in Fig. 4. The Figure revealed that the unsupported ZnO exhibits positive surface charge at pH values lower than ~9.2 (pH_{pzc} of ZnO), and that the surface positive charge increase as the pH decreases. The ZnO surface is negatively charged at pH values higher than ~9.2 where the negative charge

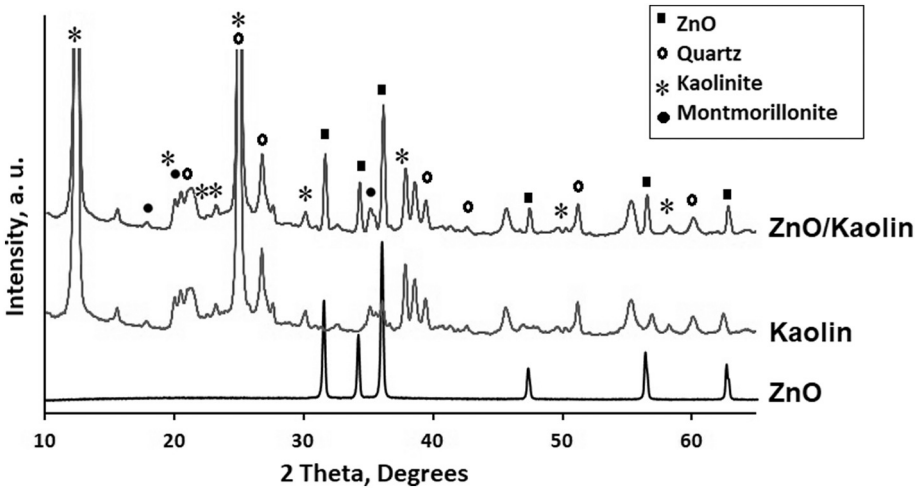

Fig. 1. X-ray diffraction patterns measured for different pre-annealed solids: ZnO, kaolin, and ZnO/Kaolin.

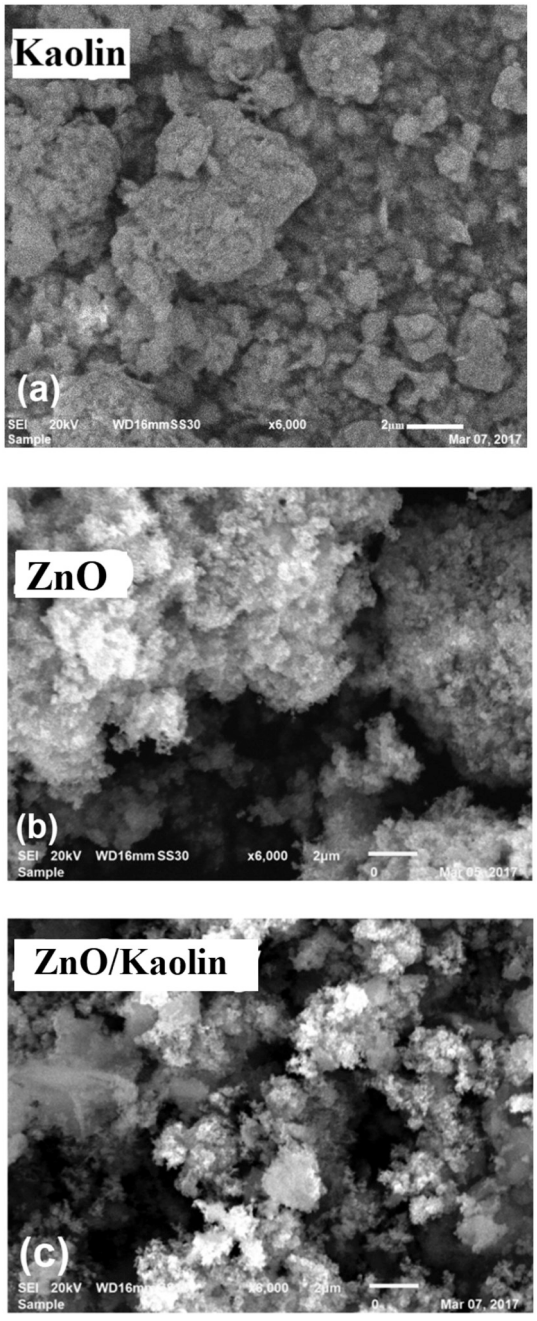

Fig. 3. Scanning electronic micrographs measured for different pre-annealed solid systems.

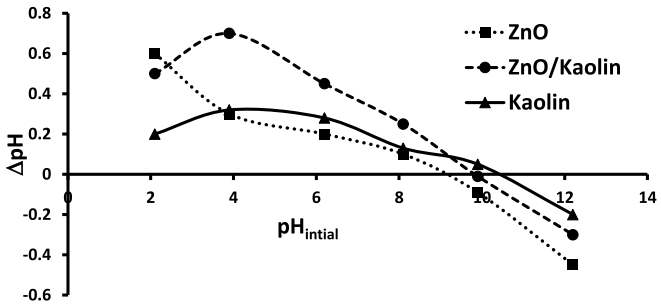

Fig. 4. Plots of Δ(pH) vs. pH measured for pre-annealed soilids ZnO, kaolin and ZnO/Kaolin. Intercepts show values of pH_{pze} for different solids. Measurements were made at 25 ± 1 °C.

Table 1
Approximate values of mass percentage for different elements present in dried clay and pre-annealed clay (kaolin)[a].

Element	Mass percentage	
	Dried	Annealed
Si	14.0	17.3
Al	7.0	8.6
Fe	1.0	1.2
Ca	8.0	10.0
Mg	2.0	2.5
Mn	0.2	0.3
K	0.4	0.6
Na	0.3	0.4
O[b]	~30–42	~37–53
C and organic contaminants[c]	~18.0	< 1.0
Others	~7–19	~6–20

[a] The values shown here are more realistic than earlier reported (da Silva Favero et al., 2016) where the clay involves values of elemental analysis reaching 99% and 100% while excluding oxygen.
[b] Oxygen was calculated based on mole ratio for oxides of Si, Al, Ca and Mg.
[c] Determined based on TGA value difference (temperature range 300–550 °C) between dried and annealed samples.

surface density increases with increased pH. The kaolin showed pH_{pzc} at pH = ~10.5, where the kaolin surface charge is positive at pH lower then ~10.5 (pH_{pzc} of kaolin), and negative at pH higher than ~10.5. The composite system ZnO/Kaolin showed a pH_{pzc} at pH ~10.0, with a positively charged surface at pH 10.0 or lower, and negatively charged surface at pH higher than ~10.0.

3.1.5. Clay elemental analysis, porosity and TG analysis results

Values of elemental analysis for clay dried at 120 °C and for the annealed one at 450 °C (Kaolin) are summarized in Table 1. The results confirm loss of organic matter in the kaolin system.

Porosity was measured using water absorption method described earlier (Franklin, 1979). The measured porosity value for pre-annealed Kaolin was ~21% by volume.

Based on measured TGA profiles for temperature range 25–900 °C, Fig. 5a, total mass loss of 10% was observed for the pre-annealed kaolin sample. The ~2% mass loss below 100 °C is due to evaporation of adsorbed humidity. The 2.5% mass loss in temperature range (100–200 °C) is attributed to coordinated water removal. The 5.5% mass loss at temperatures above 200 °C is attributed to partial decomposition of clay components, carbonates and others (da Silva Favero et al., 2016; Donoso et al., 2010; Janbuala and Wasanapiarnpong, 2015).

The 120 °C dried clay sample showed total 24% mass loss at different stages, Fig. 5b. The 5% mass loss at low temperature (< 200 °C) is attributed to adsorbed and coordinated water removal. The ~18% mass loss in the temperature range (300–550 °C) is attributed to carbon and organic contaminant burning. The other ~1% mass loss is attributed to partial clay decomposition.

3.2. Adsorption and photodegradation results

Adsorption of TC on the three pre-annealed solids (ZnO, kaolin and ZnO/Kaolin) has been studied here. The TC solutions were adjusted to specific pH values. After adsorption equilibrium (120 min) the mixture was exposed to solar simulated light for photodegradation study. The ability of solid to adsorb TC affects photodegradation by keeping the TC contaminant molecules closer to the ZnO particles.

3.2.1. Effect of pH on TC adsorption and photodegradation by ZnO

The ability of unsupported ZnO to adsorb TC at different pH values was studied, as described in Fig. 6. No observable TC loss due to adsorption at different pH values (3.1, 5.5, 7.2, 8.8, and 11.3) for 2 h,

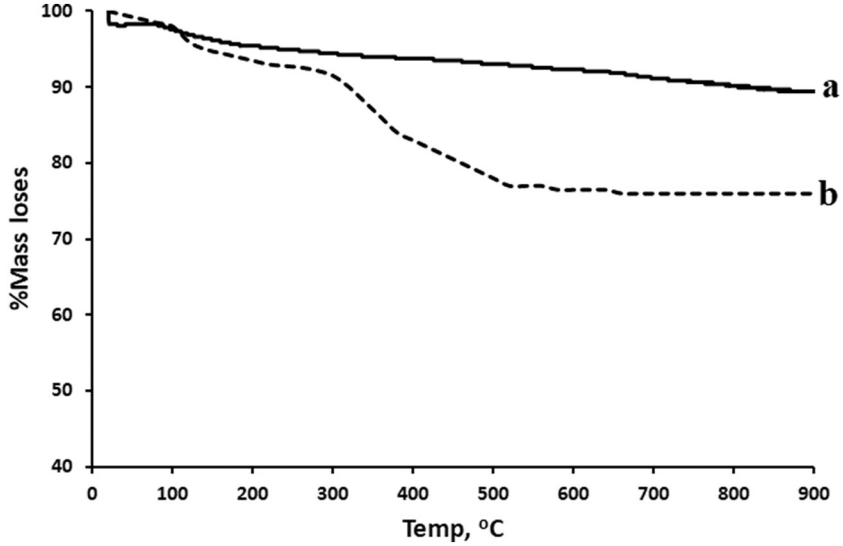

Fig. 5. Thermogravimetric analysis (TGA) profile measured for clay samples a) Pre-annealed kaolin and b) dried samples.

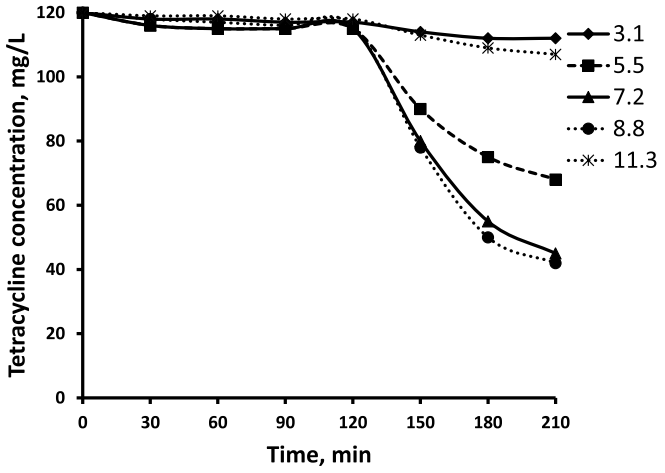

Fig. 6. Effect of pH on adsorption and photodegradation of tetracycline using ZnO nanopowder. Profiles show remaining tetracyclene concentrations with time. Concentration lowering is due to adsorption (untill 120 min) and due to photodegradation after adsorption. Experiments were made using tetracycline (100.0 mL, 120 ppm) and ZnO (0.20 g) at 25 ± 1 °C.

Fig. 6. The small adsorption ability is attributed to the small specific surface area for unsupported ZnO (~14 m^2/g). Photodegradation reaction was then undertaken on the mixture of TC (100.0 mL, 120 ppm) by exposing it to solar simulated light. Effect of pH on the photodegradation reaction progress is shown in Fig. 6. The photodegradation process is affected by the pH_{pzc}, the ZnO surface charge and TC equilibrium structure, Fig. 6. Higher photodegradation efficiency is observed at pH 7.2 and 8.8. At lower or higher pH values, the reaction goes slower. Fig. 7 describes how TC structure and ZnO surface charges vary with pH. At pH 7.2 and 8.8 the TC involves negatively charged ions, Fig. 7a, while the ZnO surface still has partially positive charges, Fig. 7b. Therefore, attractions between opposite charges kept the TC species in close proximity to the ZnO surface. This makes the TC species more susceptible to the electro-active (·OH) radicals that resulted from photoexcitation of the ZnO particles. The radicals are believed to be responsible for contaminant photodegradation in water (Lops et al., 2019). At higher pH (pH > 11) the negatively charged TC species were repelled by the negatively charged ZnO surface, which kept the contaminant species far away from (·OH) radicals. Consequently, the photodegradation process goes lower at higher pH.

At lower pH value (pH ~ 3.1), the ZnO surface charge was positive, and the TC was equilibrated as neutral to positively charged ions, Fig. 7a. The charge similarity with ZnO surface kept the TC molecules (ions) far away from ZnO surface. The photocatalytic efficiency is thus lowered. At pH = 5.5 the ZnO surface charge is positive and the TC is equilibrated in neutral form, and there is no attraction or repulsion between the TC molecules and ZnO surface. This kept the photocatalytic efficiency moderate. After photodegradation reaction cessation, desorption results showed that the adsorbed TC molecules on the ZnO surface were totally mineralized, Table 3.

3.2.2. Effect of pH on TC adsorption and photodegradation by koalin

Pre-annealed clay (Kaolin) readily adsorbed TC. The adsorption profiles at different pH values are shown in Fig. 8. Maximum TC adsorption on kaolin occurs at pH 8.8. Out of 120 ppm nominal TC solution, only 58 ppm remains un-adsorbed. The uptake capacity for the kaolin at pH 8.8 is thus 31 mg/g (51.7%). At pH 8.8 (< pH_{pzc} of kaolin ~10), the kaolin surface is positively charged and the TC was equilibrated as negatively charged, Fig. 7a. This contrariness in charge made the attraction between the kaolin surface and TC favourable. At pH 3.1 the TC was equilibrated as positively charged to neutral molecules, Fig. 7a, and kaolin surface was positively charged, Fig. 4. The similarity in charge between TC molecules and kaolin surface lowers the adsorption. At pH 11.3 the TC was equilibrated as negatively charged, Fig. 7a, and the kaolin surface was negatively charged. The similarity in charge between TC and kaolin surface lowered the adsorption. At pH 7.2 the TC is equilibrated between slightly negative to neutrally charged molecules, Fig. 7a, and the kaolin surface was positively charged, which increases TC adsorption. At pH 5.5, where the TC is equilibrated as totally neutral, Fig. 7a, and the kaolin surface was positively charged, less attraction or repulsion occurred between TC and kaolin surface.

Small loss of TC under photodegradation conditions, when using kaolin, is attributed to metal oxide composition of clay which may exhibit semiconductor photodegradation ability. The loss due to photodegradation results, at different pH values, is shown in Table 3. Most adsorbed TC was recovered by desorption process with DMSO solvent.

3.2.3. Effect of pH on TC adsorption and photodegradation by ZnO/Koalin

The adsorption and photodegradation process profiles for TC on pre-annealed ZnO/Kaolin, at different pH values, are shown in Fig. 9. The optimal pH for TC adsorption and photodegradation on ZnO/Kaolin was 8.8. At this pH, the TC was equilibrated as negatively charged

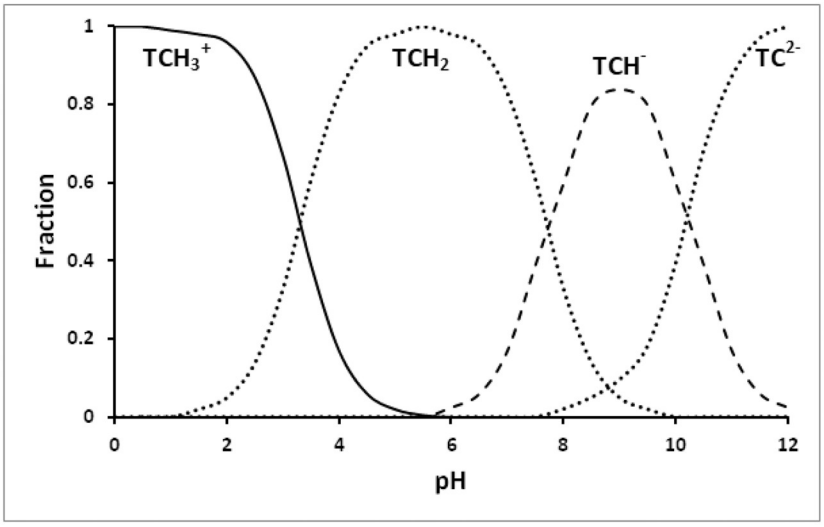

a)

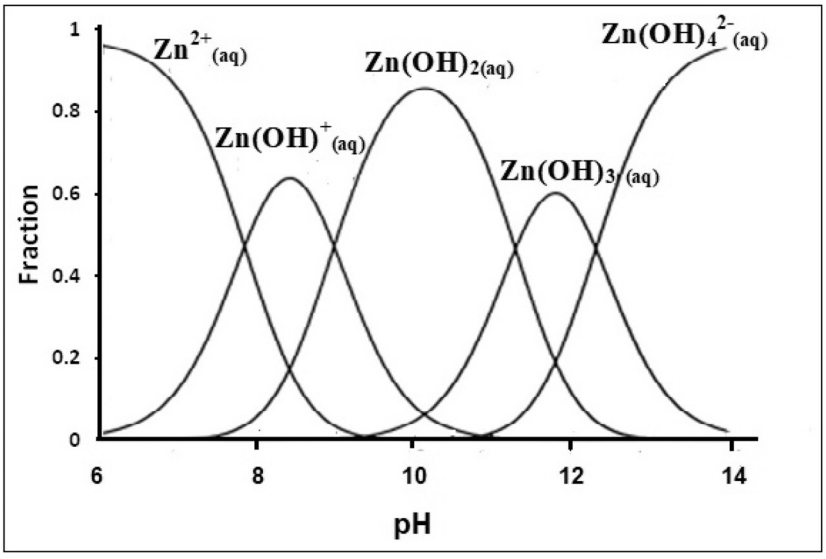

b)

Fig. 7. Effect of pH on a) tetracycline structure and b) the ZnO surface charge. Drawings are made based on known literature.

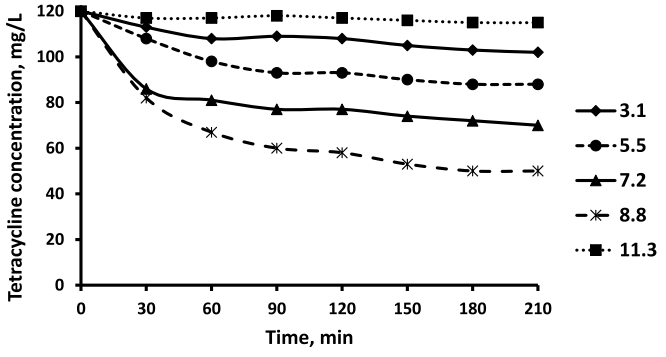

Fig. 8. Effect of pH on adsorption and photodegradation of tetracycline using kaolin. Profiles show remaining tetracyclene concentrations with time. Concentration lowering is due to adsorption (untill 120 min) and due to photodegradation after adsorption. Experiments were made using tetracycline (100.0 mL, 120 ppm) and kaolin (0.20 g) at 25 ± 1 °C.

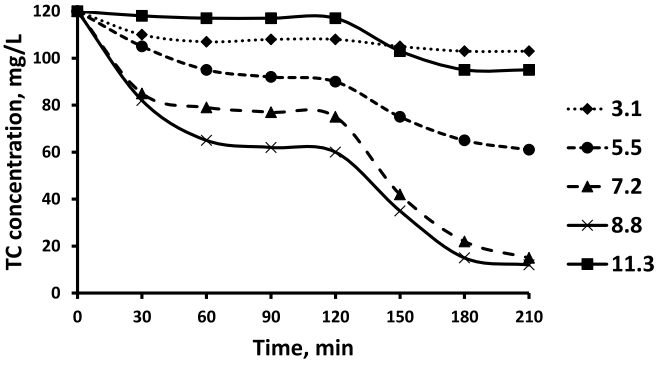

Fig. 9. Effect of pH on adsorption and photodegradation of tetracycline using pre-annealed ZnO/Kaolin. Profiles show remaining tetracyclene concentrations with time. Concentration lowering is due to adsorption (untill 120 min) and due to photodegradation after adsorption. Experiments were made using tetracycline (100.0 mL, 120 ppm) and ZnO/Kaolin (0.20 g) at 25 ± 1 °C.

Table 2
Values of TC %Loss by photodegradation using pre-annealed ZnO, kaolin and ZnO/Kaolin compared to literature.

Entry	Catalyst	Reaction time of irradiation (min.)	Contaminant initial conc, (ppm)	TC %Loss	References
1	ZnO (pH 8.8)	90	120	65	This work
2	ZnO/Kaolin (pH 8.8)	90	120	90	This work
3	Kaolin (pH 5.5)	90	120	6.7	This work
4	ZnO/Mt. Non annealed	75	120	94	(Zyoud et al., 2017)
5	ZnO/Mt. annealed	75	120	94	(Zyoud et al., 2017)
6	Mt	75	40	–	(Zyoud et al., 2017)
7	ZnO, UV	70	90	90	(Wang et al., 2016)

Table 3
Values of tetracycline adsorption, total %Loss, desorption and net photodegradation using different pre-annealed solid systems (ZnO, kaolin, ZnO/Kaolin) under different conditions[a].

	pH	Adsorption		Loss amount		Desorption		Net photo-degradation	
		(mg/g)	%Loss	(mg/g)	%Loss	(mg/g)	%Loss	(mg/g)	%Loss
ZnO	3.1	1.5	2.5	4	6.7	–	–	4	6.7
	5.5	2.5	4.2	26	43.3	–	–	26	43.3
	7.2	2.5	4.2	37.5	62.5	–	–	37.5	62.5
	8.8	2	3.3	39	65	–	–	39	65
	11.3	1	1.7	6.5	11	–	–	6.5	11
Kaolin	3.1	6	10	9	15	6.5	11	2.5	4.2
	5.5	8.5	14.2	16	26.7	14	23.3	4	6.7
	7.2	21.5	35.8	25	41.7	22	36.7	3	5
	8.8	31	51.7	35	58.	32.5	54.2	2.5	4.2
	11.3	1.5	2.5	2.5	4.2	1.5	2.5	1	1.7
ZnO/Kaolin[b]	3.1	6	10	8.5	14.2	1	1.7	7.5	12.5
	5.5	15	25	29.5	49.2	1.5	2.5	28	46.7
	7.2	27.5	45.8	52.5	87.5	2.5	4.2	50	83.3
	8.8	30	50	54	90	2.5	4.2	51.5	85.8
	11.3	1.5	2.5	12.5	20.8	2	3.3	10.5	17.5
Cut-off filter	8.8	27.5	46	38.5	64.2	3	5	35.5	59

[a] At 25 ± 1 °C.
[b] No cut-off filter used.

Table 4
Confirmation of complete mineralization of tetracycline, by total organic carbon (TOC) values and HPLC peak areas, using ZnO/Kaolin. The reaction was conducted using tetracycline (100.0 mL, 120 ppm) and ZnO/Kaolin (0.2 g) with pH ~8.8 at 25 ± 1 °C.

	TOC analysis		HPLC analysis	
Time	TOC (ppm)	%Loss	HPLC (μV sec)	%Loss
0	24	0	1,989,738	0
60	11	54	884,510	56
120	3.5	85	218,588	89
150	2	92	164,117	92

(TCH$^-$), and the ZnO/Kaolin surface was positively charged. This charge contrariness increases TC adsorption. At pH 8.8, 50% of the nominal TC concentration was adsorbed. At the end of photodegradation experiment, up to 90% TC loss was achieved. Only 4.2% of the adsorbed TC was recovered un-degraded, which confirms that photo-degradation involved the adsorbed TC molecules, Table 3. The pH 7.2 also showed superiority in adsorption and photodegradation of TC on ZnO/Kaolin, Fig. 9. At this pH, the TC was equilibrated as negatively (TCH$^-$) to neutral form (TCH_2). The negatively charged molecules readily adsorb on the positively charged ZnO/Kaolin surface. The amount of desorbed TC molecules, after the photodegradation experiment, was small (~5 ppm). This means that the adsorbed TC molecules were also photodegraded. At pH 5.5 shows moderate ability towered adsorption and photodegradation. At this pH the TC was equilibrated as neutral (TCH_2), and the ZnO/Kaolin was positively charged, which makes TC

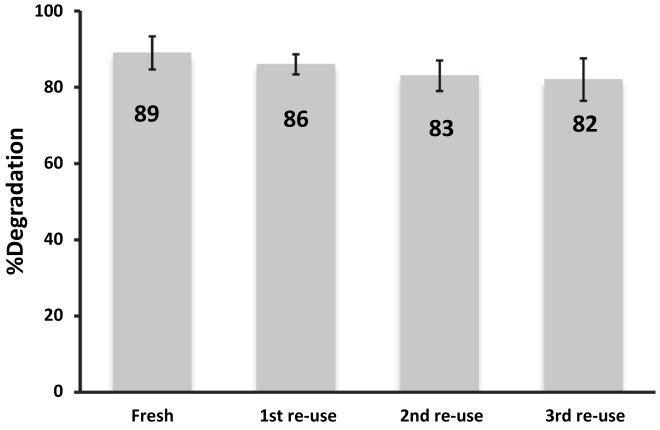

Fig. 10. Retention of photocatalytic effeciency for pre-annealed ZnO/Kaolin after recovery and reuse. Experiments were conducted by addinig fresh tetracycline (100.0 mL, 120 ppm) to the catalyst at 25 ± 1 °C at pH 8.8. Nominal fresh catalyst was 0.2 g.

molecules adsorbed moderately at the solid surface. At pH = 3.1 the TC was equilibrated between positive (TCH_3^+) and neutral (TCH_2) structures, the similarity in charges between the TC and ZnO/Kaolin surface charge keeps the TC molecules far away and lowers adsorption, and consequently photodegradation. At pH ~11.3, the TC structure was equilibrated between negatively charged structures (TC^{2-} and TCH^-), while the ZnO/Kaolin was negatively charged. The charge similarity

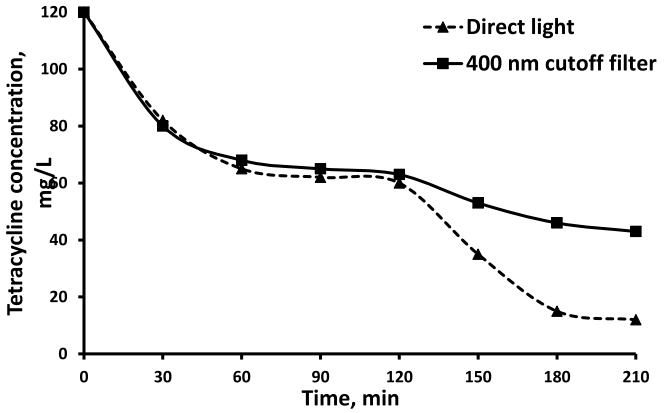

Fig. 11. Ability of tetracycline to self-sensitize its photodegradation. Profiles show adsorption (within 120 min) and followed by photodegradation of tetracycline (100.0 mL, 120 ppm) with ZnO/Kaolin (0.2 g) at 25 ± 1 °C and pH 8.8. Loss of tetracyclene with cut-off filter confirms sensitization of ZnO by tetracycline.

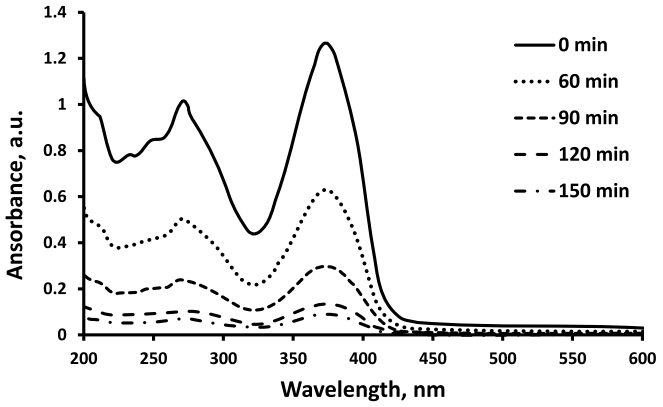

Fig. 12. Confirmation of complete mineralization of tetracycline by electronic absorption spectra. Plots show different spectra measured for aliquots of photodegradation reaction mixture with time. The reaction was conducted using tetracycline (100.0 mL, 120 ppm) and ZnO/Kaolin (0.2 g) with pH ~8.8 at 25 ± 1 °C.

increases repulsion and kept the molecules far away, and consequently reduced the photodegradation.

The ZnO/Kaolin catalyst system exhibits sound efficiency in mineralizing TC in water, as shown in Table 2. The TC %Loss exhibited by ZnO/Kaolin is significantly higher than those by unsupported ZnO or kaolin, entries (1–3). This is due to ability of the kaolin support to enhance photocatalytic efficiency by adsorbing TC molecules and bringing them into close proximity with ZnO active sites. Ability of clay support to adsorb TC molecules, at the working pH (8.8) is confirmed in Section (3.2.1.). The results show the added value of supporting ZnO onto kaolin support for TC photodegradation.

Entries (2 & 4–7) indicate that commercial Montmorillonite is a slightly superior support, than kaolin, for ZnO in TC photodegradation. This is due to montmorillonite higher adsorptivity (Uddin, 2018). However, taking into consideration the cost difference between commercial montmorillonite and kaolin, the slightly lower activity of ZnO/Kaolin here should not be considered as disadvantage for using kaolin.

3.2.4. Catalyst recovery and reuse

Naked ZnO nanoparticles cannot be easily isolated from the photodegradation reaction mixtures, due to small size. The ZnO/Kaolin composite catalyst was easily isolated by simple decantation and then reused in new photocatalytic experiments. In each reuse experiment, the recovered catalyst (< 0.20 g due to loss in handling) was mixed with fresh TC solution (100.0 mL, 120 ppm) at pH 8.8. Recovery and reuse experiments were repeated three times. The results are shown in Fig. 10. No significant loss in the catalyst efficiency occurs after the fourth use. Lowering in TC %loss in Fig. 10 is due to loss of supported catalyst during handling. The results show the added value of using

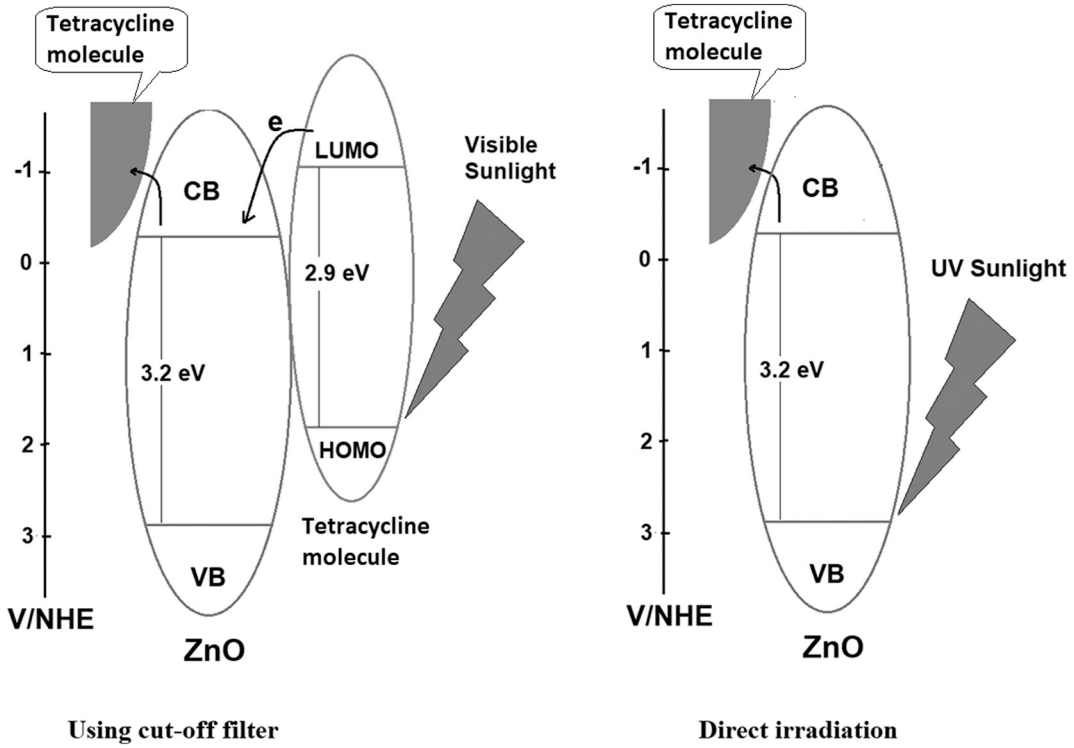

Scheme II. Schematic description showing how tetracycline (TC) molecules sensitize supported ZnO particles to visible radiations.

kaolin as support for ZnO in TC removal by photocatalysis, where the catalyst can be recovered for multiple use in future applications.

3.2.5. TC sensitization of pre-annealed ZnO/Kaolin

The ability of TC contaminant to sensitize ZnO/Kaolin catalyst to visible light was assessed here. The reaction progress profiles vs. time, with and without a cut-off filter are shown in Fig. 11. After adsorption equilibrium is reached, about 60% of nominal TC was removed when exposed to visible light within 90 min. In the absence of the cut-off filter, a higher proportion (92%) of the TC was removed, Fig. 11.

In the case of the cut-off filter, photodegradation was restricted to visible solar light. As ZnO needs UV radiation which removed by the filter, this means that the adsorbed TC molecules, with yellow color, were responsible for sensitizing the ZnO particles to visible light.

In the case of direct radiation, with no cut-off filter, the TC loss was higher (92%). In this case, two concurrent processes occur. Photodegradation by sensitized ZnO/Kaolin (in the visible region) occurs on one hand. On the other hand, photodegradation by the UV tail (~5%, available in the solar simulated radiation readily occurs. These ideas are explained in Scheme II.

3.3. Confirmation of TC complete mineralization

All reacted TC molecules were completely mineralized by photodegradation. This was confirmed using different methods. The electronic absorption spectra, Fig. 12, showed continued lowering in absorption band in the region 300–400 nm that is attributed to n-π* of hetero atoms in TC. Lowering in absorption band in the range 200–300 nm, attributed to aromatic, C═O and C═C bonds (Skoog et al., 2017) was also observed. Thus, no aromatic compounds result during photodegradation reaction. Total organic carbon (TOC) results, measured for the reaction dispersion, Table 4, further confirm complete TOC mineralization. TOC values measured after reaction cessation were consistent with HPLC analysis values for unreacted TC contaminant.

4. Conclusion

ZnO nanoparticles catalyze photodegradation of TC in water with UV tail in solar simulated light. When supported onto kaolin particles, the efficiency of ZnO particles increases due to adsorption. Compared to fresh sample, the supported catalyst retained its catalytic efficiency with no significant loss after third reuse. The ability of the yellow TC molecules to sensitize supported ZnO particles is confirmed, which means that the supported catalyst can function in the visible range. Complete mineralization of reacted TC molecules, by photodegradation, is confirmed by various methods. Zero point charge study shows that the supported ZnO catalyst efficiency is affected by pH value of the medium. Optimal pH range is ~6–9 which shows the possibility of using the ZnO/Kaolin as an effective catalyst for TC mineralization under natural conditions (room temperature and pH 8.8). The results show the feasibility of using ZnO/Kaolin in future water purification processes using natural solar radiations.

Author contributions

A.H.Z. and H.S·H formulated the work ideas and the manuscript writing up. A.H.Z and A.Z. performed lab experiments. S.Z, N.Q. and AR.H performed SEM and XRD measurements at UAE University. M.H. helped with the literature review and TC drug concepts. Sh.Z. measured TOC. All Authors read and approved the manuscript.

Declaration of Competing Interests

The authors declare that they have no competing interests.

This research did not receive any specific grant from funding agencies in the public, commercial, or not-for-profit sectors.

Appendix A. Supplementary data

Supplementary data to this article can be found online at https://doi.org/10.1016/j.clay.2019.105294.

References

Adamson, A.W., Gast, A.P., 1967. Physical Chemistry of Surfaces. Interscience, New York.
Agwuh, K.N., MacGowan, A., 2006. Pharmacokinetics and pharmacodynamics of the tetracyclines including glycylcyclines. J. Antimicrob. Chemother. 58, 256–265.
Ashraf, K.M., Khan, M.R.K., Higgins, D.A., Collinson, M.M., 2018. pH and Surface Charge Switchability on Bifunctional Charge Gradients. Langmuir 34, 663–672.
Chantes, P., Jarusutthirak, C., Danwittayakul, S., 2015. A comparison study of photocatalytic activity of TiO2 and ZnO on the degradation of Real Batik Wastewater, International Conference on Biological, Environment and Food Engineering (BEFE-2015). Int. Inst. Chem. Biol. Environ. Eng. 15–16.
Choudhury, B., Borah, B., Choudhury, A., 2012. Extending photocatalytic activity of TiO2 nanoparticles to visible region of illumination by doping of cerium. Photochem. Photobiol. 88, 257–264.
da Silva Favero, J., Parisotto-Peterle, J., Weiss-Angeli, V., Brandalise, R.N., Gomes, L.B., Bergmann, C.P., dos Santos, V., 2016. Physical and chemical characterization and method for the decontamination of clays for application in cosmetics. Appl. Clay Sci. 124, 252–259.
Deepracha, S., Bureekaew, S., Ogawa, M., 2019. Synergy effects of the complexation of a titania and a smectite on the film formation and its photocatalyst'performance. Appl. Clay Sci. 169, 129–134.
Diamond, S., Kinter, E.B., 1956. Surface areas of clay minerals as derived from measurements of glycerol retention. Clay Clay Miner. 5, 334–347.
Donoso, J.P., Tambelli, C., Magon, C.J., Mattos, R., Silva, I., Souza, J., Moreno, M., Benavente, E., Gonzalez, G., 2010. Nuclear magnetic resonance study of hydrated bentonite. Mol. Cryst. Liq. Cryst. 521, 93–103.
Franklin, J.A., 1979. Suggest methods for determining water content, porosity, density, absorption and related properties and swelling and slake-durability index properties. Int. J. Rock Mech. Min. Sci. Geomech. Abstr. 16, 141–156.
Hadjltaief, H.B., Galvez, M.E., Zina, M.B., Da Costa, P., 2014. TiO2/clay as a heterogeneous catalyst in photocatalytic/photochemical oxidation of anionic reactive blue 19. Arab. J. Chem. https://doi.org/10.1016/j.arabjc.2014.11.006.
Hamilton, R.J., Rowley, A.K., 2009. Book Review: Tarascon Pocket Pharmacopoeia: 2009 Deluxe Lab-Coat Pocket Edition. SAGE Publications Sage CA, Los Angeles, CA.
Hilal, H.S., Nour, G.Y., Zyoud, A., 2009. Photo-degradation of methyl orange with direct solar light using znoand activated carbon-supported Zno. In: Water Purification. Novascience Pub, NY.
Hussien, E.M., 2014. Development and validation of an HPLC method for tetracycline-related USP monographs. Biomed. Chromatogr. 28, 1278–1283.
Janbuala, S., Wasanapiarnpong, T., 2015. Effect of rice husk and rice husk ash on properties of lightweight clay bricks. Key Eng. Mater. 74–79.
Ju, H., Jiang, Y., Xue, B., Xu, Y., Guo, H., Huo, M., Li, F., 2018. UV shielding performance of illite/TiO 2 nanocomposites. New J. Chem. 42, 9260–9268.
Kumar, H.D., Häder, D.-P., 1999. Solar ultraviolet radiation. In: Global Aquatic and Atmospheric Environment. Springer, pp. 341–376.
Kümmerer, K., 2009. Antibiotics in the aquatic environment–a review–part I. Chemosphere 75, 417–434.
Kuo, S.L., Liao, C.J., 2006. Solar Photocatalytic Degradation of 4-Chlorophenol in Kaolinite Catalysts. J. China Chem. Soc-Taip 53, 1073–1083.
Liu, Z.-D., Zhou, Q., Hong, Z.-N., Xu, R.-K., 2017. Effects of surface charge and functional groups on the adsorption and binding forms of Cu and Cd on roots of indica and japonica rice cultivars. Front. Plant Sci. 8, 1489.
Lops, C., Ancona, A., Di Cesare, K., Dumontel, B., Garino, N., Canavese, G., Hérnandez, S., Cauda, V., 2019. Sonophotocatalytic degradation mechanisms of Rhodamine B dye via radicals generation by micro-and nano-particles of ZnO. Appl. Catal. B-Environ. 243, 629–640.
Miao, X.-S., Bishay, F., Chen, M., Metcalfe, C.D., 2004. Occurrence of antimicrobials in the final effluents of wastewater treatment plants in Canada. Environ. Sci. Technol. 38, 3533–3541.
Moan, J., 2001. Visible light and UV radiation. In: Radiation at Home, Outdoors and in the Workplace. Scandinavian Publisher, Oslo, pp. 69–85.
Morkel, J., Kruger, S., Vermaak, M., 2006. Characterization of clay mineral fractions in tuffisitic kimberlite breccias by X-ray diffraction. J S Afr. I Min. Metall. 106, 397–406.
Nasiruddin Khan, M., Sarwar, A., 2007. Determination of points of zero charge of natural and treated adsorbents. Surf. Rev. Lett. 14, 461–469.
Noh, J.S., Schwarz, J.A., 1989. Estimation of the point of zero charge of simple oxides by mass titration. J. Colloid Interf. Sci. 130, 157–164.
Organization, W.H., 2015. 19th WHO Model List of Essential Medicines (April 2015). WHO, Geneva.
Osabor, V., Okafor, P., Ibe, K., Ayi, A., 2009. Characterization of clays in Odukpani, south eastern Nigeria. Afr. J. Pure Appl. Chem. 3, 079–085.
Ruiz-Hitzky, E., Aranda, P., Akkari, M., Khaorapapong, N., Ogawa, M., 2019. Photoactive nanoarchitectures based on clays incorporating TiO2 and ZnO nanoparticles. Beilstein J. Nanotech. 10, 1140–1156.
Sakthivel, S., Neppolian, B., Shankar, M., Arabindoo, B., Palanichamy, M., Murugesan, V., 2003. Solar photocatalytic degradation of azo dye: comparison of photocatalytic efficiency of ZnO and TiO2. Sol. Energy Mater. Sol. C 77, 65–82.
Santhosh, C., Malathi, A., Daneshvar, E., Kollu, P., Bhatnagar, A., 2018. Photocatalytic degradation of toxic aquatic pollutants by novel magnetic 3D-TiO 2@ HPGA

nanocomposite. Sci. Rep. Uk 8, 15531.
Shoemaker, D.P., Garland, C.W., Nibler, J.W., Feigerle, C.S., 1996. Experiments in Physical Chemistry. McGraw-Hill, New York.
Skoog, D.A., Holler, F.J., Crouch, S.R., 2017. Principles of Instrumental Analysis. Cengage Learning.
Szabó, T., Németh, J., Dékány, I., 2003. Zinc oxide nanoparticles incorporated in ultrathin layer silicate films and their photocatalytic properties. Colloid Surf. A 230, 23–35.
Uddin, F., 2018. Montmorillonite: An Introduction to Properties and Utilization. Current Topics in the Utilization of Clay in Industrial and Medical Applications. pp. 1.
Umar, A., Ribeiro, C., Al-Hajry, A., Masuda, Y., Hahn, Y., 2009. Growth of highly c-axis-oriented ZnO nanorods on ZnO/glass substrate: growth mechanism, structural, and optical properties. J. Phys. Chem. C 113, 14715–14720.
Wang, H., Yao, H., Pei, J., Liu, F., Li, D., 2016. Photodegradation of tetracycline antibiotics in aqueous solution by UV/ZnO. Desalin. Water Treat. 57, 19981–19987.
Xiang, C., Yang, F., Li, M., Jaridi, M., Wu, N., 2013. Experimental and statistical analysis of surface charge, aggregation and adsorption behaviors of surface-functionalized titanium dioxide nanoparticles in aquatic system. J. Nanopart. Res. 15, 1293.
Xu, X.-R., Li, X.-Y., 2010. Sorption and desorption of antibiotic tetracycline on marine sediments. Chemosphere 78, 430–436.
Yogendra, K., Naik, S., Mahadevan, K., Madhusudhana, N., 2011. A comparative study of photocatalytic activities of two different synthesized ZnO composites against Coralene Red F3BS dye in presence of natural solar light. Int. J. Environ. Sci. Res. 1, 11–15.
Zyoud, A.H., Hilal, H.S., 2009. Silica-supported CdS-sensitized TiO2 particles in photo-driven water purification: Assessment of efficiency, stability and recovery future perspectives. In: Water Purification. Novascience Pub, NY in Press, 2008.
Zyoud, A.H., Zaatar, N., Saadeddin, I., Ali, C., Park, D., Campet, G., Hilal, H.S., 2010. CdS-sensitized TiO2 in phenazopyridine photo-degradation: Catalyst efficiency, stability and feasibility assessment. J. Hazard. Mater. 173, 318–325.
Zyoud, A., Zaatar, N., Saadeddin, I., Helal, M.H., Campet, G., Hakim, M., Park, D., Hilal, H.S., 2011. Alternative natural dyes in water purification: anthocyanin as TiO2-sensitizer in methyl orange photo-degradation. Solid State Sci. 13, 1268–1275.
Zyoud, A., Zu'bi, A., Helal, M.H., Park, D., Campet, G., Hilal, H.S., 2015. Optimizing photo-mineralization of aqueous methyl orange by nano-ZnO catalyst under simulated natural conditions. J. Environ. Health Sci. 13, 46.
Zyoud, A., Dwikat, M., Al-Shakhshir, S., Ateeq, S., Shteiwi, J., Zu'bi, A., Helal, M.H., Campet, G., Park, D., Kwon, H., 2016a. Natural dye-sensitized ZnO nano-particles as photo-catalysts in complete degradation of E. coli bacteria and their organic content. J. Photochem. Photobiol. A 328, 207–216.
Zyoud, A., Jondi, W., Mansour, W., Khan, M.M., Hilal, H.S., 2016b. Modes of tetra (4-pyridyl) porphyrinatomanganese (III) ion intercalation inside natural clays. Chem. Cent. J. 10, 12.
Zyoud, A., Jondi, W., AlDaqqah, N., Asaad, S., Qamhieh, N., Hajamohideen, A., Helal, M.H., Kwon, H., Hilal, H.S., 2017. Self-sensitization of tetracycline degradation with simulated solar light catalyzed by ZnO@ montmorillonite. Solid State Sci. 74, 131–143.
Zyoud, A., Zorba, T., Helal, M., Zyoud, S., Qamhiya, N., Hajamohideen, A., Zyoud, S., Hilal, H., 2019. Direct sunlight-driven degradation of 2-chlorophenol catalyzed by kaolinite-supported ZnO. Int. J. Environ. Sci. Technol. 1–10.